Harmonic Analysis and Active Filtering in Offshore Wind Power Plants

S. K Chaudhary, F. D. Freijedo, J. M. Guerrero, R. Teodorescu and C. L. Bak
Department of Energy Technology
Aalborg University,
Aalborg, Denmark

Ł. H. Kocewiak
DONG Energy Wind Power,
Fredericia, Denmark

C. F. Jensen
Energinet.dk,
Fredericia, Denmark

***Abstract*— Due to presence of long high voltage cable networks, and power transformers for the grid connection, the offshore wind power plants (OWPPs) are susceptible to harmonic distortion and resonances. The grid connection of OWPP should not cause the harmonic distortion beyond the permissible limits at the point of common coupling (PCC). The resonance conditions should be avoided in all cases.**

This paper describes the harmonic analysis techniques applied on an OWPP network model. A method is proposed to estimate the harmonic current compensation from a shunt-connected active power filter to mitigate the harmonic voltage distortion at the PCC. Finally the harmonic distortions in the compensated and the uncompensated systems are compared to demonstrate the efficacy of the compensation.

Keywords-harmonic distortion, offshore wind power plant, driving point impedance, transfer impedance, resonance, active filter.

I. INTRODUCTION

Offshore wind power plants (OWPP) are a promising source of renewable energy. The electrical infrastructure of a typical OWPP includes hundreds of wind turbine (WTs) connected to the collector grid by a widespread medium voltage (MV) cable network [1]-[3]. Eventually the OWPP is connected to the onshore AC grid using long high voltage (HV) export cables and transformers. The presence of long cable network and the transformers lead to low-frequency resonances in the network [2]. Further, the distributed nature of the cable shunt capacitance and its series inductance leads to multiple resonant frequencies. When a harmonic source is present around the resonant frequency, there can be amplification of the harmonic voltage and/or current. Such a situation has to be avoided by proper analysis, design and harmonic mitigation plans.

While the network impedance characteristic imposes resonance conditions and potential amplification of harmonic distortion, there has to be a source which would excite the resonance or create harmonic voltage distortions in the first place. In an OWPP, the harmonic source could be the onshore grid itself or the wind turbines [4]. Potential resonance conditions and harmonic distortion in a power system network can be studied using harmonic analysis tools like the frequency scan and the harmonic power-flow [2], [5].

This work is supported by Energinet.dk through the project "Active filter functionalities for power converters in wind power plants" (Forskel program, project number PSO-2014-1-12188).

Passive filters are widely used for the filtering of undesirable harmonics. An active power filters has significant advantages over the passive filters as it allows for continuous and adaptive tuning to cope with the changing network configurations, and the same filter might be tuned to compensate for several frequency components [6].

This paper presents the harmonic analysis of an OWPP network model and then applies the harmonic current compensation to mitigate the 11^{th} and 13^{th} harmonic distortion. The harmonic impedance characteristic is used to estimate the compensating currents and to demonstrate its effect on other bus in the network. Only the effect of background grid harmonics have been analyzed here.

II. TEST NETWORK MODEL

Anholt OWPP is used here as the reference for developing the benchmark WPP model [1]. It is a 400 MW OWPP comprising of 111 SWT-3.6-120 WTs. It is connected to the 400 kV grid at the onshore substation at Trige via two units of 400/220 kV, 450 MVA auto-transformers. The export cable comprises of 58 km aluminum 3x1x2000 mm^2 underground cable and 24.5 km 3x1600 mm^2 sub-marine cable. The reactive power compensation is provided by 240 MVAr reactors at 220kV onshore transformer terminals and 120 MVAr reactor in between the onshore and offshore cable sections. There are three 140 MVA, 220/33 kV plant step-up transformers as shown in Fig. 1. The collector grid has a total cable length of 152 km at 33 kV. Two potential locations of the active power filter at the bus T1 and T2 are shown as well.

The grid is modelled as a Thévenin voltage source with series impedance. The grid impedance exhibits a frequency dependent characteristic. First the amplification of the harmonic distortion is shown using 1% harmonic distortion in the background grid from the 2^{nd} to the 20^{th} harmonic orders Afterwards a realistic spectrum of background harmonics is applied and the harmonic analysis is performed.

III. HARMONIC ANALYSIS

Harmonic frequency scan (also known as Frequency sweep) gives the harmonic impedance characteristics at different buses in the network. It indicates the potential resonant frequencies. A high impedance magnitude at a

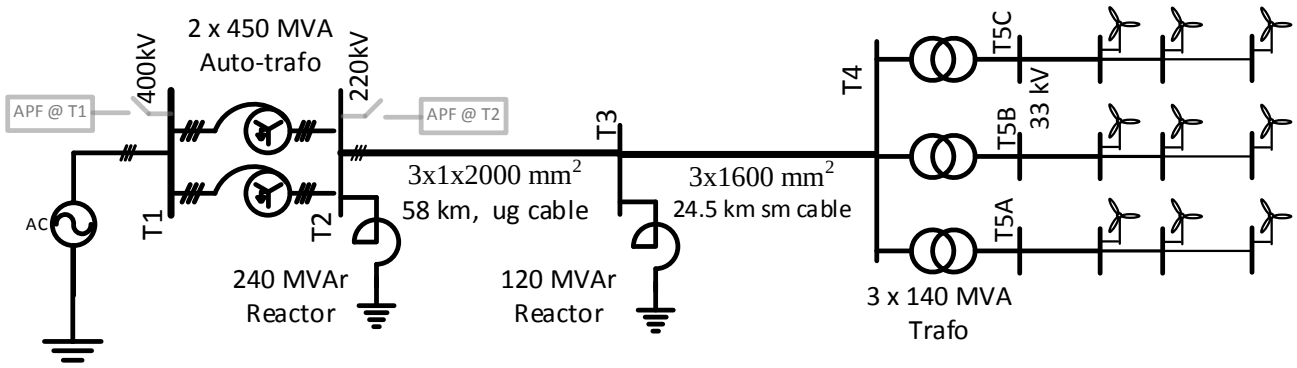

Fig. 2. WPP electrical network model.

particular frequency indicates the appearance of the parallel resonance at that frequency. Similarly, a low impedance characteristic indicates potential series resonance at that frequency. Apart from this, the total impedance changes from inductive to capacitive or vice versa at the resonant frequencies. This appears as change of sign of the impedance phase angle.

The harmonic analysis tool in DigSILENT, provides the driving point impedance at different buses and transfer impedance between the selected bus pairs in the system.

A. *Driving point impedance versus frequency characteristics*

Harmonic driving point impedance at the bus *k* for the harmonic order *h* is defined as the bus voltage appearing at that particular bus, when unit current is injected at that bus. Mathematically, it is written as,

$$\overline{Z_{hk}} = \frac{\overline{V_{hk}}}{\overline{I_{hk}}} \qquad (1)$$

where, $\overline{Z_{hk}}$ is the driving point impedance, and $\overline{V_{hk}}$ is the harmonic voltage appearing, due to the current $\overline{I_{hk}}$ injected at bus *k*. All these are complex numbers and the subscript '*h*' indicates the harmonic order. Thus, the harmonic driving point impedance indicates the harmonic voltage controllability by the injection of harmonic current at a particular bus. The driving point impedance information can be used in determining the harmonic current injection for the compensation of harmonic voltage distortion at the specific bus. It is the diagonal term in the bus-impedance matrix.

The harmonic driving point impedance in sequence components at the PCC bus T1 is shown in Fig. 2. The impedance at the fundamental frequency is 22.6 Ω at 83.5°. The series resonances are characterized by low impedances value of 1 Ω at 800, 874 and 985 Hz as shown in Fig. 2. At 176 Hz, the impedance is 11 Ω. Likewise, parallel resonances are indicated by very high impedance values of 117 Ω, 528 Ω, 113 Ω, and 125 Ω at 114, 450, 515, and 947 Hz respectively.

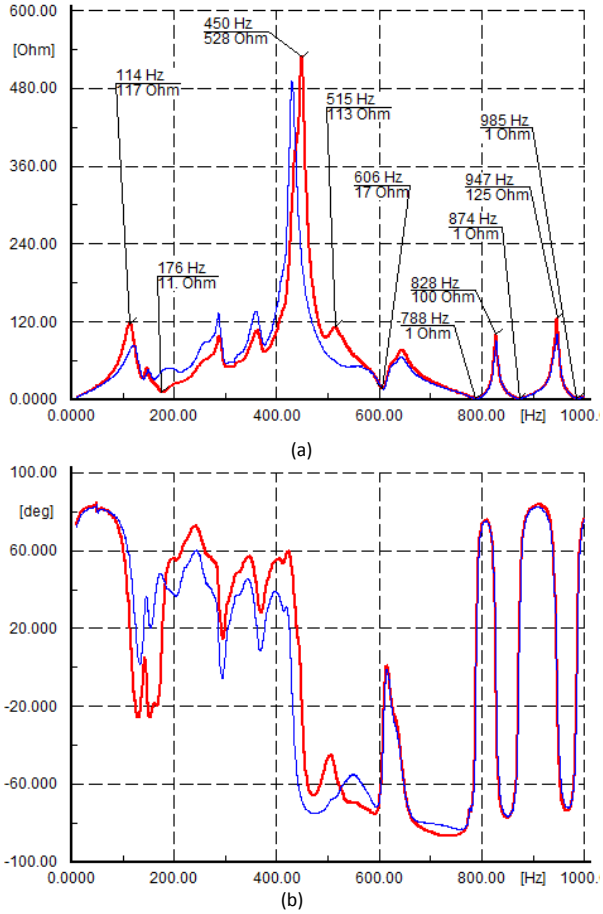

Fig. 1. Positive and negative sequences (thick, red) and zero sequence (thin, blue) components of the driving point impedance at the bus T1 (a) Magnitude. (b) Phase.

B. *Transfert impedance versus frequency characteristics*

Harmonic transfer impedance, between any two terminals in the network, is defined as the voltage appearing at the first bus, when unit current is injected at the second bus. These are the off-diagonal terms in the bus impedance matrix. Mathematically, it can be written as,

$$\overline{Z_{hab}} = \frac{\overline{V_{ha}}}{\overline{I_{hb}}}. \qquad (2)$$

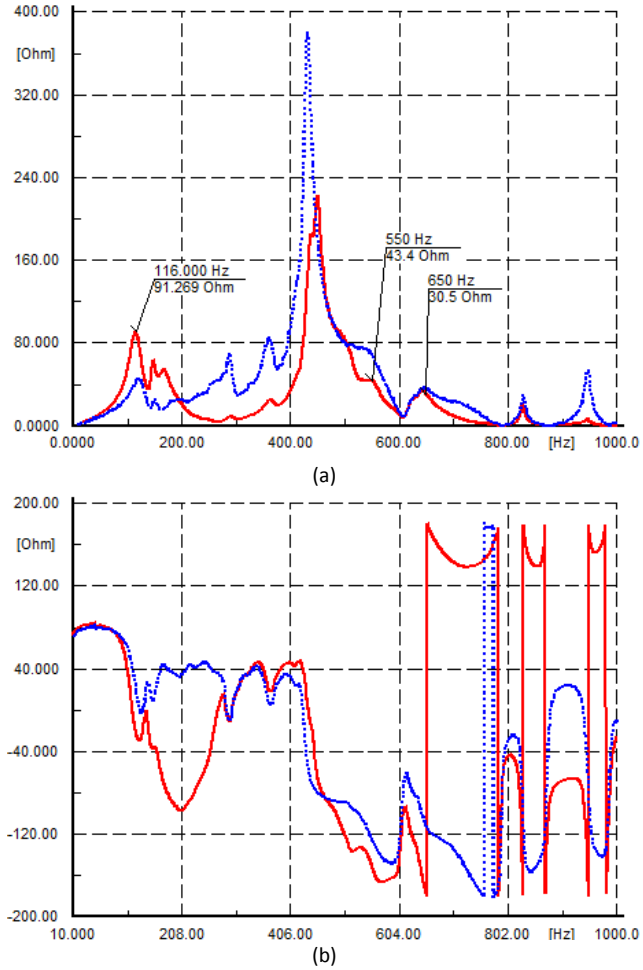

Fig. 3. Positive and negative sequences (thick, red) and zero sequence (dotted, blue) components of the transfer impedance between bus T1 and T2 (a) Magnitude. (b) Phase.

Here, $\overline{Z_{hab}}$ is the transfer impedance between the bus pair *A*↔*B*, and $\overline{V_{ha}}$ is the voltage appearing at bus *A*, due to the current $\overline{I_{hb}}$ injected at bus B. Thus, the harmonic transfer impedance between a pair of buses indicates the harmonic voltage controllability at the first bus by the injection of harmonic current at the second bus which is relevant for active filter optimal dimensioning and placement within the electrical infrastructure. Therefore, if local harmonic compensation is estimated by (1), its effect on another bus can be estimated using the transfer impedance. For instance, if at bus *b*, the compensating current for the *h*-th harmonic is estimated by using the relation (1), its impact on bus *a* will be given by,

$$\Delta\overline{V_{ha}} = \overline{Z_{hab}}\overline{I_{hb}} = \frac{\overline{Z_{hab}}}{\overline{Z_{hb}}}\overline{V_{hb}}\,. \tag{3}$$

The transfer impedance between a pair of buses is reciprocal magnitude when it is expressed in Ω. It is reciprocal in phase as well, if there is not any phase shifting transformer between the selected pair of buses. The actual effect of local harmonic compensation on the harmonic distortion at another can be estimated by using the phase relationship of (3), i.e.,

$$\left|\delta_{ha} - \delta_{hb} - \theta_{hab} + \theta_{hb}\right| \le \frac{\pi}{2}, \tag{4}$$

where, δ is the phase angle of the voltage, and θ is the phase angle of the impedance. The subscript *h* indicates the harmonic order, and the subscript *a* or *b* indicates the bus number. The double subscript *ab* indicate the pair of buses for the transfer impedance.

The transfer impedance between the bus-pairs T2↔T1 is given in Fig. 3. The maximum value of 220 Ω appears at 449 Hz. It is observed that the magnitude of the transfer impedance is reciprocal to each other in magnitude for any pair of buses, even when there is a phase shifting transformer in between them. Sudden jumps in the curves for the phase angles of the transfer impedances appear due to the change of angle from (-180˚) to (+180˚).

C. Harmonic voltage amplification

To determine the voltage amplification, due to a specific source of distortion at a given bus *k* in the network, the network can be divided into two parts as shown in Fig. 4. The harmonic voltage at the bus *k* is given by,

$$V_{hk} = \frac{Z_{lh}}{Z_{sh}+Z_{lh}} V_{sh} \tag{5}$$

Thus, the voltage amplification factor is $\left(\frac{Z_{lh}}{Z_{sh}+Z_{lh}}\right)$. It tends to be higher than 1, when there are both capacitive and reactive elements in the network, which leads to a smaller denominator, i.e. $|Z_{sh} + Z_{lh}| < |Z_{lh}|$.

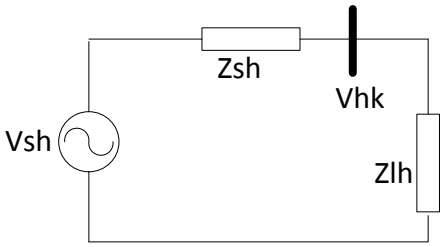

Fig. 4. Equivalent network for the harmonic voltage at bus *k*.

At the resonant frequency, $Z_{sh} + Z_{lh} = 0$ as the reactive impedance gets cancelled by the capacitive impedance and hence there is a very low resistive impedance, leading to a high current magnitude. In the case of parallel resonance, the reactive and capacitive impedances appear in parallel, and hence the total impedance is very high.

D. Harmonic distortion

Harmonic power-flow analysis computes the harmonic voltages and hence the harmonic voltage distortion at different buses in the network. At first, 1% harmonic distortion is assumed in the background grid at all the harmonics orders up to the 20th order The harmonic distortion in the network, with none of the WTs connected,

is shown in Fig. 5. There is harmonic voltage amplification at bus T1 (i.e. harmonic voltage higher than 1%) for the orders 2nd, 10th to 15th, 17th and the 19th. The second harmonic voltage is amplified at all four buses under study; in fact the amplification factor increases as we proceed towards the bus T4. The 4th harmonic also gets amplified at the buses T3 and T4.

However, such a uniform background harmonic does not usually appear in power systems. A realistic harmonic spectrum of the background harmonics and the corresponding distortion is shown in Fig. 6. The background harmonic spectrum in the inset (a) shows the prominence of the 3rd, 5th, 7th, 11th, 13th, and the 19th harmonic orders. The harmonic power-flow analysis result shows the amplification of harmonic voltage distortion at the 11th, 13th, and the 19th harmonic orders. Out of these, only the 11th and the 13th order harmonics are chosen for compensation due to the fact that they tend to be the most prominent in the analyzed system. The 19th order harmonic has not been considered here though it can be compensated in a similar way if the converter control bandwidth is sufficient.

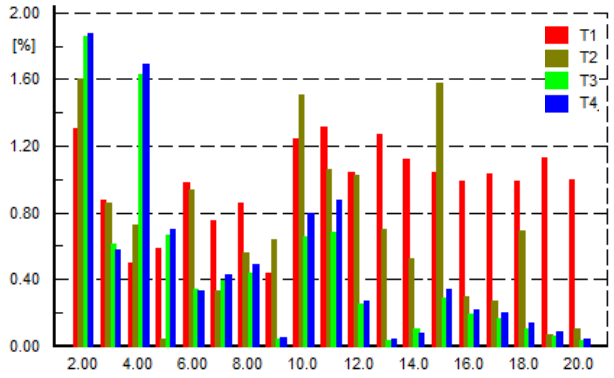

Fig. 5. Harmonic distortion at the bus T1, T2, T3 and T4 for 1% background harmonics in the grid.

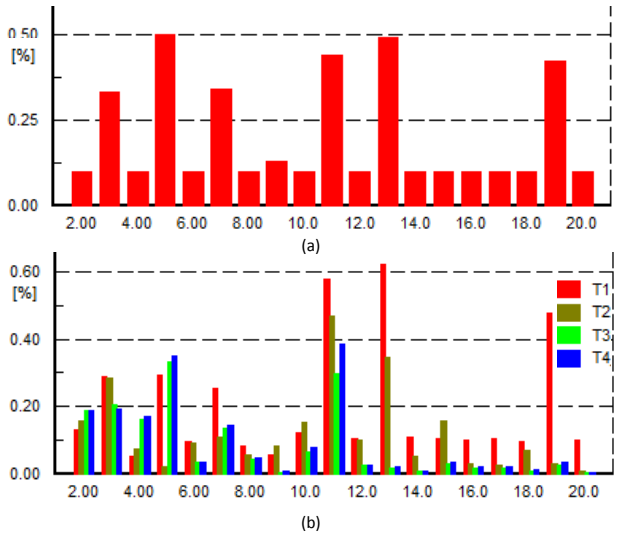

Fig. 6. (a)Background harmonic voltage distortion in the grid. (b) Harmonic distortion at the bus T1, T2, T3 and T4 due to the background harmonics in the grid.

TABLE I. HARMONIC COMPENSATING CURRENTS

Comp. Bus	Harm. Order	Phase A		Phase B		Phase. C	
		Mag.	Ph.	Mag.	Ph.	Mag.	Ph.
T1	11	20 A	84°	18 A	206°	16 A	314°
	13	20 A	72°	19 A	313°	20 A	199°
T2	11	9 A	232°	9 A	22°	8 A	180°
	13	7 A	246°	7 A	151°	12 A	17°

TABLE II. SEQUENCE COMPONENTS OF THE HARMONIC COMPENSATING CURRENTS

Comp. Bus	Harm. Order	Positive		Negative		Zero	
		Mag.	Ph.	Mag.	Ph.	Mag.	Ph.
T1	11	2. A	76°	18 A	82°	1 A	170°
	13	20 A	75°	1 A	30°	0. A	279°
T2	11	3 A	148°	8 A	263°	2 A	216°
	13	9 A	258°	3 A	136°	1 A	11°

TABLE III. HARMONIC COMPENSATING CURRENTS FOUND BY ITERATIVE ANALYSIS

Comp. Bus	Harm. Order	Positive		Negative		Zero	
		Mag.	Ph.	Mag.	Ph.	Mag.	Ph.
T1	11	x	x	16 A	85°	X	x
	13	19 A	74°	X	x	X	x
T2	11	x	x	8 A	272°	X	X
	13	9 A	274°	x	X	x	X

IV. HARMONIC CURRENT COMPENSATION

An ideal harmonic compensator is designed on the basis of (1) for mitigating the amplification of the 11th and the 13th harmonic components at the buses T1 and T2. The objective is to inject harmonic currents into T1 or T2 that would cancel out the harmonic voltages at the local bus (i.e. T1 or T2). The compensating current for phase A at bus T1 for the 11th harmonic can be computed from the corresponding line-ground voltage of 1.33 kV at the phase 14° (line-ground), and the impedance of 66 Ω at the phase −70° by,

$$I_{11,T1A} = \left(\frac{1.33*1000}{66}\right)\angle 84° = 20\angle 84°\ A \qquad (6)$$

The ideal compensating currents for the 11th and the 13th harmonic compensation provided separately at the bus T1 and T2 are shown in Table I. Since the network is unbalanced due to the layout of the underground cables in flat-formation, the harmonic impedances and the harmonic voltages are unbalanced, and hence the harmonic compensating current turns out to be unbalanced. It contains positive, negative and zero sequence components as shown in Table II. When these currents were used as reference currents for compensation at the bus T1, there was some improvement at the local bus T1 as well as in the whole system. However, the improvement was not the same for all the phases. On the other hand, when the harmonic compensation was applied at the bus T2 using the reference currents from the Table I, the distortion in phase B and C voltages was found to be worse, even at the local bus T2.

TABLE IV. COMPARISON OF HARMONIC DISTORTION (HD) AND THD IN THE UNCOMPENSATED CASE AND THE CASES WITH COMPENSATION AT T1 AND AT T2.

		T1			T2		
		Ph. A	Ph. B	Ph. C	Ph. A	Ph. B	Ph. C
HD% (11th)	Uncomp	0.58	0.46	0.44	0.47	0.89	0.47
	Comp at T1	0.01	0.01	0.01	0.01	0.02	0.01
	Comp at T2	0.56	0.56	0.57	0.01	0.01	0.01
HD% (13th)	Uncomp-	0.62	0.54	0.59	0.34	0.41	0.65
	Comp at T1	0.02	0.01	0.02	0.01	0.01	0.02
	Comp at T2	0.59	0.59	0.59	0.00	0.00	0.01
THD	Uncomp-	1.15	1.04	1.06	0.74	1.07	0.93
	Comp at T1	0.77	0.76	0.76	0.46	0.44	0.48
	Comp at T2	1.12	1.11	1.12	0.46	0.44	0.48

An iterative approach was used to find out the harmonic compensating currents which would result in the minimum distortion at the local bus. The results are tabulated in Table III. It is found that such currents are in close agreement with the negative sequence current component for the 11th harmonic order and the positive sequence component for the 13th harmonic order in Table II. This observation is in agreement with the fact that the 11th order background harmonic voltage was applied in negative sequence. The reference currents according to the Table III were applied at the bus T1 and at the bus T2 separately.

A. Harmonic current compensation at the bus T1

When the harmonic compensation is provided at T1, the harmonic voltage distortion is reduced 0.01-0.02% at the bus T1 and T2 for both the 11th and the 13th harmonics as shown in Table IV. The overall THD is also reduced at the bus T1 and T2.The improvement is observed at the buses T3 and T4 as well. The reduction in harmonic voltage distortion for phase A at the buses T1, T2, T3 and T4 due to the compensation at the bus T1 harmonic is shown in Fig. 7.

B. Harmonic current compensation at the bus T2

The harmonic current compensation at T2 leads to the harmonic reduction, at the local bus T2 and other 220 kV bus in the OWPP network. The harmonic distortion at the bus T2 is reduced to less than 0.01%. However, the same is not true for the 400 kV bus T1. Rather the results in Table IV show an increase in the harmonic distortions and the overall THD by a few percentage for the phases B and C.

Thus while the harmonic compensation at T1 benefitted led to the reduction of harmonic distortion at the bus T2, the reverse is not true. This phenomenon can be explained using (4). The net phase difference between the harmonic voltage at T2 and the voltage appearing at T2 due to the harmonic compensation at T1, computed according to (1), is 8.7°. Therefore, the compensation at T1 reduces the harmonic distortion at T2 as well. On the other hand, for the compensation at T2, the net phase difference between the harmonic voltage at T1 and the voltage induced at T1 is 210°. Hence the compensation at T2 would have, in general, a worsening effect for the harmonics at T1. Though the transfer impedance (in Ω) is reciprocal, the effect appears more pronounced at T2 than at the 400 kV bus due to the difference in the nominal voltage levels.

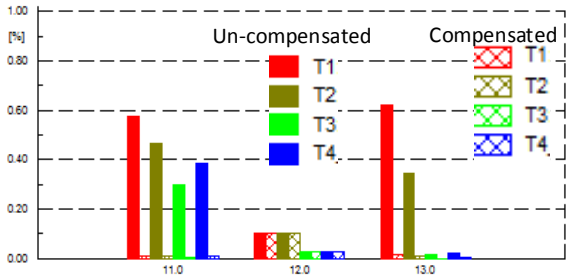

Fig. 7. Comparison of harmonic distortion in the uncompensated (solid bars) and the system with 11th and 13th harmonic current compensation (solid bars) at the bus T1.

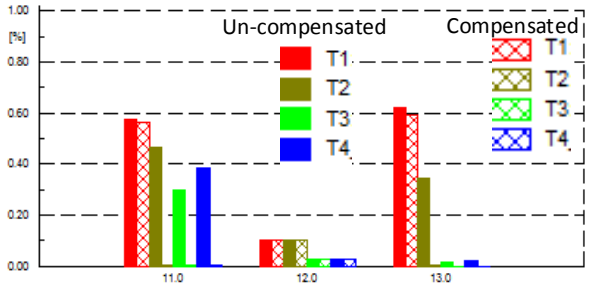

Fig. 8. Comparison of harmonic distortion in the uncompensated (solid bars) and the system with 11th and 13th harmonic current compensation (solid bars) at the bus T2.

V. CONCLUSION

The paper explains the harmonic impedance characteristics of an OWPP model and the resultant propagation and amplification of the harmonic distortions from the grid to the OWPP network. When the OWPP is connected to the grid, the harmonic impedance characteristic at the point of connection is changed. This leads to a change in harmonic distortion at the PCC. The final harmonic voltage distortion profile also depends upon the prevalent harmonics in the background spectrum.

It was found that the 11th and the 13th harmonic voltages were amplified to relatively higher levels. An idealized harmonic current compensation was been estimated using the driving point impedance and the harmonic bus voltages at the local bus. It was found the balanced compensation using the negative sequence for the 11th harmonic and positive

sequence for the 13th harmonic was more effective in reducing the harmonic distortion levels. Another contribution is the use of transfer impedance characteristic to predict the effect of harmonic compensation at one bus on another bus. It can be used to optimize the compensating currents so as to mitigate harmonic distortion at several buses in the network.

REFERENCES

[1] Ł. H. Kocewiak, B. L. Øhlenschlæger Kramer, O. Holmstrøm, K. H. Jensen and L. Shuai, "Active Filtering Application in Large Offshore Wind Farms," in International Workshop on Large-Scale Integration of Wind Power into Power Systems as well as Transmission Networks for Offshore Wind Farms, Berlin, 2014.

[2] M. Bradt, B. Badrzadeh, E. Camm, D. Mueller, J. Schoene, T. Siebert, T. Smith, M. Starke and R. Walling, "Harmonics and resonance issues in wind power plants," in IEEE PES Transmission and Distribution Conference and Exposition, Orlando, 7-10 May 2012.

[3] Ł. H. Kocewiak, S. K. Chaudhary and B. Hesselbæk, "Harmonic Mitigation Methods in Large Offshore Wind Power Plants," in The 12th International Workshop on Large-Scale Integration of Wind Power into Power Systems as well as Transmission Networks for Offshore Wind Farms, London, 2013.

[4] B. Badrzadeh and M. Gupta, "Practical Experiences and Mitigation Methods of Harmonics in Wind Power Plants," *IEEE Trans. Ind. Appl.*, vol. 49, no. 5, pp. 2279–2289, Sep. 2013.

[5] B. Badrzadeh, M. Gupta, N. Singh, A. Petersson, L. Max, and M. Hogdahl, "Power system harmonic analysis in wind power plants --- Part I: Study methodology and techniques," in IEEE Industry Applications Society Annual Meeting (IAS), 2012.

[6] Ł. H. Kocewiak, S. K. Chaudhary, and B. Hesselbæk, "Harmonic Mitigation Methods in Large Wind Farms," in *Wind Integration Workshop, London*, 2013, no. June, p. 2013.